Patagonia Icefield melting observed by Gravity Recovery and Climate Experiment (GRACE)

J. L. Chen,[1] C. R. Wilson,[1,2] B. D. Tapley,[1] D. D. Blankenship,[3] and E. R. Ivins[4]

[1] Using recently released reprocessed gravity solutions from the Gravity Recovery and Climate Experiment (GRACE), we estimate the ice loss rate for the Patagonia Icefield (PIF) of South America, for the period April 2002 through December 2006. After postglacial rebound and hydrological effects are corrected, the estimated rate is -27.9 ± 11 km^3/year, equivalent to an average loss of ~ -1.6 m/year ice thickness change if evenly distributed over the entire PIF area. The estimated contribution to global sea level rise is 0.078 ± 0.031 mm/year. This is an independent confirmation of relatively large melting rate estimates from earlier studies employing topographic and cartographic data. **Citation:** Chen, J. L., C. R. Wilson, B. D. Tapley, D. D. Blankenship, and E. R. Ivins (2007), Patagonia Icefield melting observed by Gravity Recovery and Climate Experiment (GRACE), *Geophys. Res. Lett.*, *34*, L22501, doi:10.1029/2007GL031871.

1. Introduction

[2] The Patagonia Icefield (PIF) is the second largest ice body in the Southern Hemisphere [*Warren and Sudgen*, 1993] and consists of a Northern Patagonia Icefield (NPI), with an area $\sim$4200 km^2 in Chile and a Southern Patagonia Icefield (SPI), with an area $\sim$13000 km^2 within Chile and Argentina [*Rignot et al.*, 2003] (see Figure 1). There is evidence of historical and contemporary melting and retreat of glacial ice within the PIF. *Rignot et al.* [2003] compared topographic data and estimated total NPI and SPI ice loss of about 15.0 ± 0.8 km^3/year for the period 1968/1975–2000. An estimate for 1995–2000, in the same study [*Rignot et al.*, 2003] for the PIF (NPI + SPI) ice loss rate was about 37.7 ± 4.0 km^3/year, suggesting an acceleration of melting rate. Another study [*Aniya et al.*, 1997] analyzed various remote sensing data (including aerial photographs, Landsat, and SPOT data) from 1944/1945 and 1985/1986 and estimated ice loss in the SPI for this period in the range of 126 to 342 km^3. The corresponding range of annual rates is 3.1 to 8.3 km^3/year. *Rignot et al.* [2003] estimated an SPI mass loss rate of about $\sim$12.2 $\pm$ 0.7 km^3/year for the period 1968/1975 until 2000. The 2007 Intergovernmental Panel on Climate Change report shows that cumulative losses in

Patagonia since 1960 are approximately 40 m of ice thickness averaged over the glaciers [*Lemke et al.*, 2007].

[3] Estimates of ice loss for NPI and SPI are difficult to obtain for several reasons, including a lack of observations with adequate spatial and temporal sampling. The relatively small size, steep slopes, and complicated geography of both the NPI and SPI limit the utility of remote sensing techniques, such as laser or radar altimetry and interferometric synthetic aperture radar (InSAR). Here we estimate the ice loss rate using changes in Earth's gravity field observed from space by the Gravity Recovery and Climate Experiment (GRACE). Since its March 2002 launch, GRACE has provided monthly gravity fields of unprecedented accuracy [*Tapley et al.*, 2004]. Changes in gravity fields from month to month provide a fundamental measure of mass redistribution. GRACE data have been used in a number of geophysical applications, including estimation of continental water storage change [e.g., *Wahr et al.*, 2004], global sea level change [e.g., *Chambers et al.*, 2004; *Lombard et al.*, 2007], polar ice sheet melting [e.g., *Velicogna and Wahr*, 2006; *Chen et al.*, 2006; *Ramillien et al.*, 2006], and Alaskan mountain glacier melting [e.g., *Tamisiea et al.*, 2005].

[4] Early GRACE gravity fields such as the release 1 solutions (denoted as RL01) were contaminated by various noise artifacts, especially in the higher degree and order spherical harmonics (SH). As a result, spatial resolution was no better than about 500 to 1000 km, depending on data processing details, geographic latitude and the time scale of the variation [*Wahr et al.*, 2004]. A very recent GRACE data set, the release 4 (denoted as RL04) offers significantly improved spatial resolution due to improved background geophysical models used in GRACE data processing, and is suitable for estimating ice loss rates for areas as small as the PIF. As demonstrated in a recent study [*Chen et al.*, 2007], spatial resolution on the order of 300 km is possible with RL04 solutions when estimating changes over time scales of a year and longer.

2. Data Processing and Results

2.1. GRACE Observed Long-Term Mass Change in Patagonia

[5] From 53 monthly GRACE RL04 gravity solutions, covering the period April 2002 to December 2006, we use GRACE SH coefficients (up to degree and order 60) to compute monthly global mass change fields on a 1° × 1° grid. The details of the upgrades and/or geophysical background models used in the RL04 GRACE solutions are given by *Bettadpur* [2007]. As demonstrated by *Swenson and Wahr* [2006], the GRACE stripping noise is due to the correlation among the even or odd degree SH coefficients at

---
[1]Center for Space Research, University of Texas at Austin, Austin, Texas, USA.

[2]Department of Geological Sciences, University of Texas at Austin, Austin, Texas, USA.

[3]Institute for Geophysics, University of Texas at Austin, Austin, Texas, USA.

[4]Jet Propulsion Laboratory, California Institute of Technology, Pasadena, California, USA.
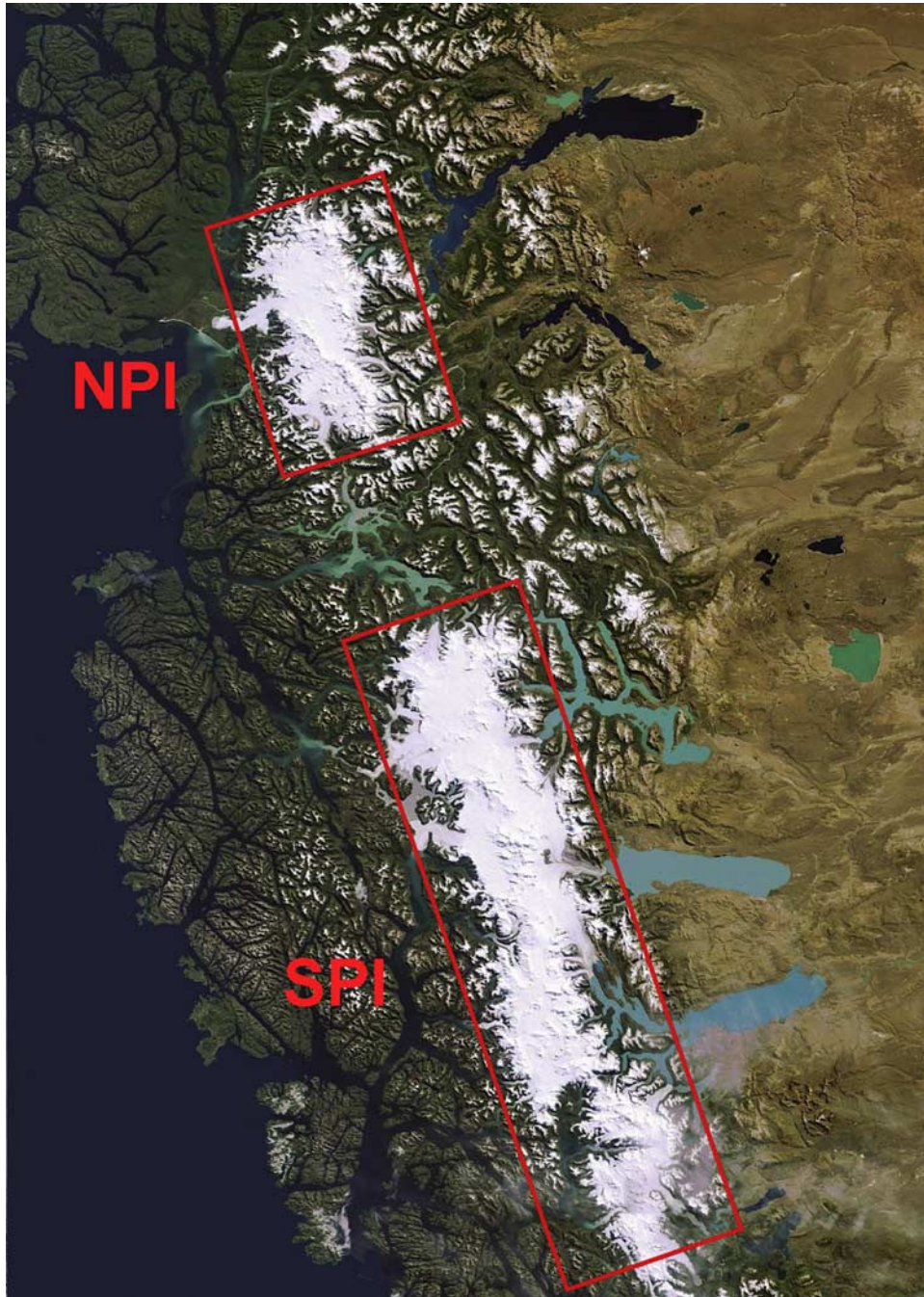
Figure 1. A satellite image of the Northern Patagonia Icefield (NPI) and Southern Patagonia Icefield (SPI) in South America, as circled by the red boxes. The original image is provided by the European Space Agency.

a given order. We apply a two-steps filtering method used in a recent study [*Chen et al.*, 2007] that first removes correlated noise at SH orders where this problem has been identified, followed by smoothing with a 300 km Gaussian filter [*Jekeli*, 1981]. For a given SH order (6 and above), we use a least squares fit to the even and odd coefficient pairs and remove a polynomial of order 4 (this processing step is denoted as P4M6). The mean of the 53 solutions is removed to obtain time series of gravity field variations.

[6] A global mass-rate map is obtained by fitting a linear trend to time series at every grid point using least squares. Seasonal (annual and semiannual) sinusoids, and a 161-day sinusoidal term are fit simultaneously. The 161-day term is recognized the primary aliasing signal in GRACE data due to the errors in semidiurnal S_2 tides [*Han et al.*, 2005], which is related to GRACE orbit configuration. As GRACE generates the monthly global gravity change map from along track satellite range and range rate data, errors in high frequency ocean tide model (used in GRACE
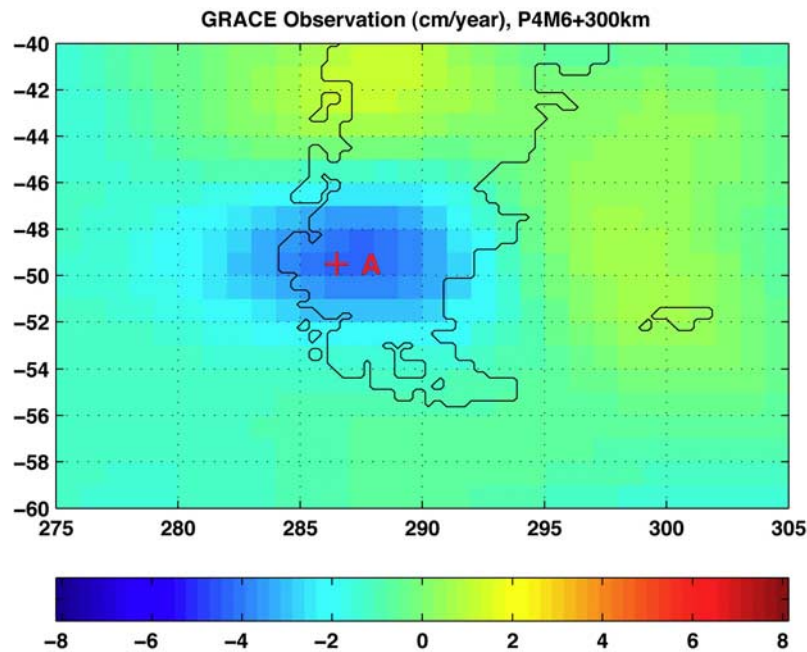
Figure 2. GRACE linear mass rates (in units of cm of equivalent water height change per year, cm/yr) for April 2002 to December 2006, in the PIF region. The 2-step filtering involves application of a decorrelation filter to remove noise stripes at certain SH orders, followed by 300 km Gaussian smoothing. Mass rates are estimated from the 53 time series values at each grid point using least squares to fit the linear trend, seasonal, and tidal alias sinusoids.

data processing) will produce artificial long-period (e.g., 161-day in this case) variability in GRACE gravity data. Figure 2 shows the mass rate map for the PIF and surrounding areas, showing a clearly negative rate centered on the PIF area. Limited spatial resolution creates a diffuse region of negative rates, as variations within the PIF leak into surrounding areas. This leakage of variance is due both to a limited range of SH coefficients, and to the applied Gaussian smoothing [e.g., *Chen et al.*, 2006]. To obtain estimates of mass loss in the PIF, we employ a forward modeling technique developed in previous studies [e.g., *Chen et al.*, 2006]. Estimates are derived assuming that the geographical location of mass change is within the PIF, and can be interpreted as due to ice melting. Other causes of mass change might contribute as well. An example might be ground water storage fluctuations in surrounding regions.

[7] Figure 3a shows (with square symbols) the time series of GRACE observed surface mass changes over the 5 years period at grid point A (within the SPI area, Figure 4). Point A is positioned on the largest glacier of SPI, Pio XI, which even experienced significant thickening (~2.2 m/year) during the period 1975–1995 [e.g., *Rivera and Casassa*, 1999]. The smooth curve shows a least squares fit of a linear trend, seasonal, and 161-day sinusoids. Figure 3b shows the residual GRACE series and linear trend after removing sinusoidal terms. The slope is -3.74 ± 0.21 cm/year of equivalent water mass.

2.2. Forward Modeling of Ice Loss Rate in PIF

[8] Figures 2 and 3 both show an apparent surface mass decrease in the PIF region, but a forward modeling calculation is required to interpret it and similar rates at surrounding grid points, in terms of mass change within the PIF as a whole [e.g., *Chen et al.*, 2006]. The modeling effort proceeds as follows:

[9] 1. We assign mass rates to the NPI and SPI rectangular regions shown in Figure 4. The mass change is distributed uniformly over the regions defined by $1° \times 1°$ grid elements. The remainder of the grid (all other points on Earth's surface outside the box circled by red lines) retains GRACE mass rates.

[10] 2. A predicted mass rate map is obtained by representing the $1° \times 1°$ grid of mass rates (constructed as in step 1) as fully normalized SH, then truncating the coefficients at degree and order 60, the same limit used in RL04. Finally we apply the same decorrelation (P4M6) and 300 km Gaussian smoothing filters used to obtain GRACE rate maps. This ensures that rate estimates are not biased by this filtering.

[11] 3. We adjust model mass rates until predicted and GRACE rate maps agree in shape and peak magnitude. The quantitative constraint is that the spatially integrated mass rate over the anomaly region (in the NPI/SPI area) is the same in both GRACE and model rate maps. Integration is a sum over grid point values with cosine of latitude weighting. The anomaly region is taken as the set of contiguous grid points (circled by white lines in Figures 5a and 5b) on the model and GRACE mass rate maps where the rate magnitude exceeds 1 cm/year equivalent mass change.

[12] Figure 5 compares mass rate maps from GRACE (Figure 5, top) and from a mass rate model that meets the outlined criteria (Figure 5, bottom). The mass rate
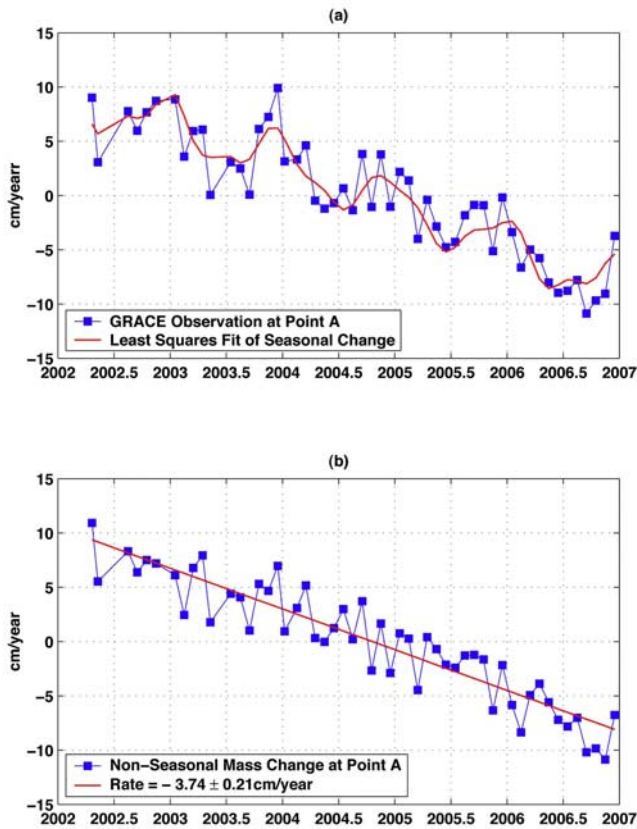
Figure 3. (a) GRACE mass changes (in blue curve with square markers) from the 53 RL04 gravity solutions at location A, marked in Figure 1. The red curve represents the least square fit of a linear trend, seasonal (annual and semiannual) sinusoids, and a 161-day tidal aliasing term. (b) Non-seasonal mass change (in blue curve with square markers) from GRACE at the same location. The red line is the linear trend from the least squares fit.

corresponds to loss of ~24.3 km^3/year of equivalent water, or an average ice loss of ~1.4 m/years over the entire NPI/SPI area. The model rate map (Figure 5, bottom) matches the GRACE rate map (Figure 5, top) well.

2.3. Other Geophysical Contributions

[13] GRACE-observed long-term mass change in the PIF region could include other contributions, e.g., interannual atmospheric and hydrological change and postglacial rebound (PGR) of the Earth mantle due to ice mass load change from the Last Glacial Maximum and present-day ice melting [*Ivins and James*, 2004; *Klemann et al.*, 2007]. Atmospheric effect has been removed through the dealiasing process in GRACE data processing using the European Center for Medium range Weather Forecasting climate model [*Bettadpur*, 2007]. We estimate possible 'apparent' long-term land water storage change in the PIF regions (i.e., the area circled by white lines in Figure 5 (bottom)) using monthly terrestrial water storage estimates from the LadWorld land surface model [*Milly and Shmakin*, 2002], during roughly the same period (April 2002 to November 2006). The LadWorld data show that terrestrial

water storage change could contribute ~−5.4 km^3/year of equivalent water to GRACE estimate.

[14] We employ a regional PGR model by *Ivins and James* [2004] (with lithosphere thickness of 65 km and sub-cratonic mantle viscosity of 1.0×10^{19} Pa s). The predicted PGR contribution is $+9 \pm 8$ km^3/year of equivalent water. The PGR uplift rate in the PIF region is highly sensitive to asthenospheric viscosity, as the PIF is located in a unique tectonic setting, and here the upper mantle viscosity is much lower than, e.g., in Fennoscandia.

3. Conclusions and Discussions

[15] From the forward modeling effort, we conclude that over the 5 years sampled by GRACE RL04 (April 2002 to December 2006), mass is lost at a rate of 24.3 ± 4.3 km^3/year in the PIF region. The standard error in the estimate is taken from the standard errors of the linear trend estimates fit to time series in this region. If we assume the uncertainty of model predicted hydrological effects is of 100% of the model prediction, and after hydrological and PGR effects are removed, GRACE-observed PIF ice melting rate is 27.9 ± 11 km^3/year. There is additional uncertainty related to misfit between model and observed rate maps, and to errors in the GRACE observations themselves, which we judge to be relatively less important. The estimated loss rate of 27.9 ± 11 km^3/year is large, considering the small size of the PIF area. The estimated contribution to global sea level rise is about 0.078 ± 0.031 mm/year. Previous estimates [*Rignot et al.*, 2003; *Aniya et al.*, 1997] are varied, but our GRACE value is comparable to the estimate derived from topographic and cartographic data [*Rignot et al.*, 2003] (-37.7 ± 4.0 km^3/year for 1995–2000). Agreement is
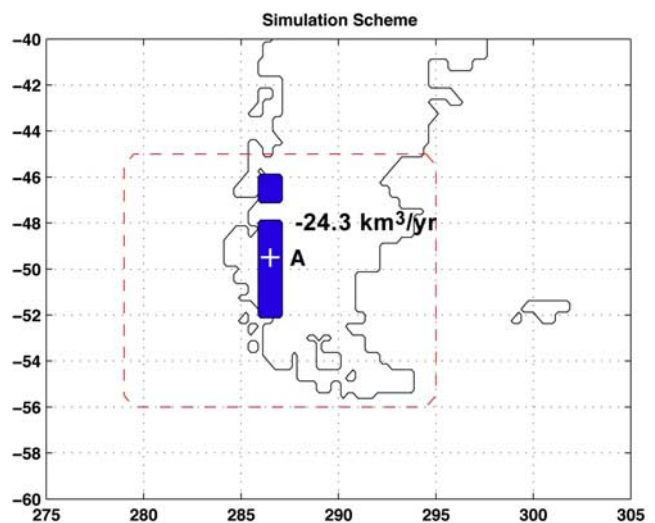

Figure 4. Illustration of the forward modeling scheme: The two shaded areas represent the NPI and SPI areas, respectively. A total mass rate of ~−24.3 km^3/year is uniformly distributed over the two shaded areas. Mass changes at grid points outside the red box are adopted from GRACE observation (as shown in Figure 2). The white cross marks point (A) for which time series are shown in Figure 3.
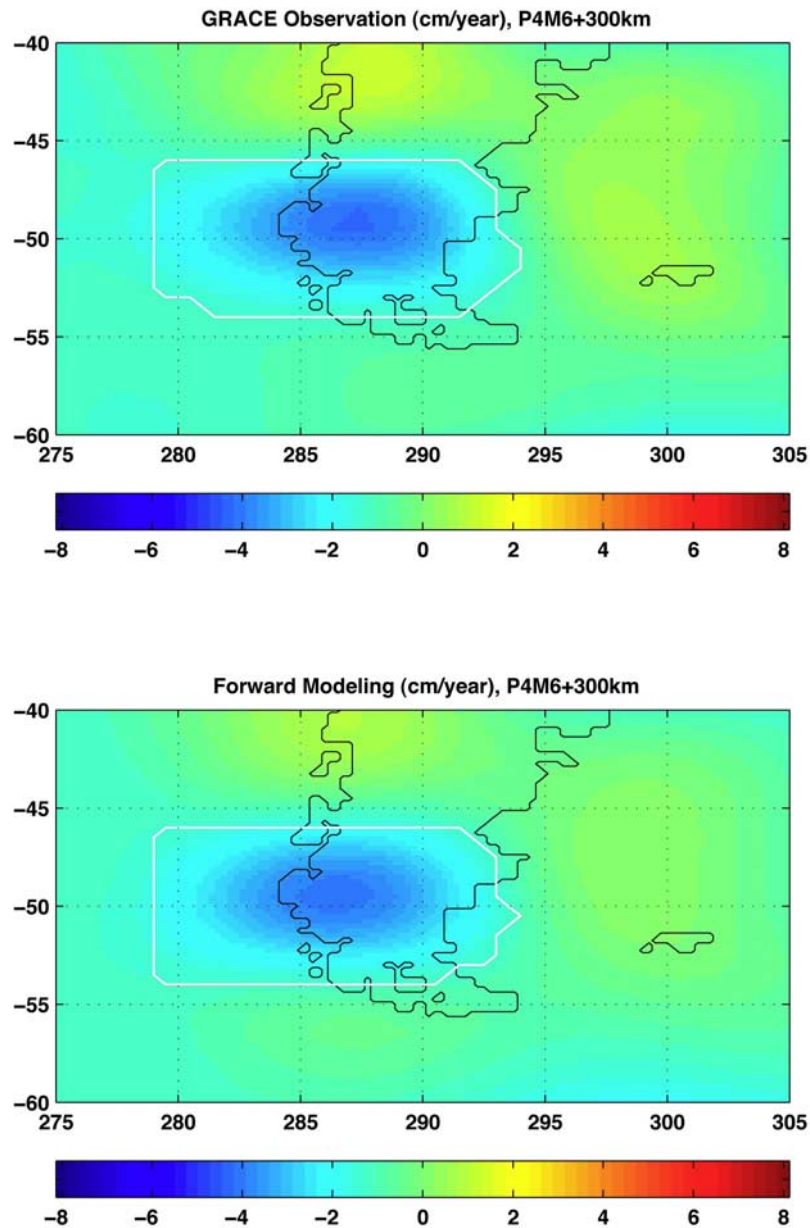
Figure 5. (top) Same GRACE observations (as in Figure 2) interpolated onto $0.25° \times 0.25°$ grids (from the original $1° \times 1°$ grid). The white lines circle the area within which rate magnitude drops below 1 cm/year, defining the anomaly region. (bottom) Forward modeling rate map prediction (also $0.25° \times 0.25°$ grids). The white lines circle the area where the rate magnitude drops below 1 cm/yr. The areas circled by white boxes are the regions in which we sum total mass rate with cosine of latitude weighting, as described in the text.

reasonable considering that there are fundamental differences in the observed quantities, that this earlier study [*Rignot et al.*, 2003] examined a different time period, and that it employed observations from only a portion of the SPI.

[16] GRACE-observed PIF ice melting rate (27.9 ± 11 km^3/year) is equivalent to an average loss of ~ -1.6 m/years ice thickness change if evenly distributed over the entire PIF area. There is significant spatial variability over the entire PIF area, with some glaciers or areas showing significant thinning [e.g., *Rivera and Casassa*, 2004; *Raymond et al.*, 2005], while others even thickening [e.g., *Rivera and Casassa*, 1999].

[17] In additional to remaining GRACE measurement errors and errors associated with the spatial filtering and forward modeling, uncertainty of model predicted PGR and interannual terrestrial water storage change in the PIF region is a major error source to our estimate. The estimated PGR uncertainty may not reflect the real error there. Steady improvement of GRACE gravity fields seen in RL04 is encouraging, and enables GRACE results to be applied to a wider class of problems than previously possible.

References

Aniya, M., H. Sato, R. Naruse, P. Skvarca, and G. Casassa (1997), Recent glacier variations in the southern Patagonia Icefield, *South Am. Arct. Alp.*, *29*(1), 1–12, doi:10.2307/1551831.

Bettadpur, S. (2007), Level-2 gravity field product user handbook, GRACE 327-734, GRACE Proj., Cent. for Space Res., Univ. of Tex. at Austin, Austin.

Chambers, D. P., J. Wahr, and R. S. Nerem (2004), Preliminary observations of global ocean mass variations with GRACE, *Geophys. Res. Lett.*, *31*, L13310, doi:10.1029/2004GL020461.

Chen, J. L., C. R. Wilson, and B. D. Tapley (2006), Satellite gravity measurements confirm accelerated melting of Greenland Ice Sheet, *Science*, *313*(5795), 1958–1960, DOI:10.1126/science.1129007.

Chen, J. L., C. R. Wilson, B. D. Tapley, and S. Grand (2007), GRACE detects coseismic and postseismic deformation from the Sumatra-Andaman earthquake, *Geophys. Res. Lett.*, *34*, L13302, doi:10.1029/2007GL030356.

Han, S.-C., C. K. Shum, and K. Matsumoto (2005), GRACE observations of M_2 and S_2 ocean tides underneath the Filchner-Ronne and Larsen ice shelves, Antarctica, *Geophys. Res. Lett.*, *32*, L20311, doi:10.1029/2005GL024296.

Ivins, E. R., and T. S. James (2004), Bedrock response to Llanquihue Holocene and present-day glaciation in southernmost South America, *Geophys. Res. Lett.*, *31*, L24613, doi:10.1029/2004GL021500.

Jekeli, C. (1981), Alternative methods to smooth the Earth's gravity field, report, Dep. of Geod. Sci. and Surv., Ohio State Univ., Columbus.

Klemann, V., E. R. Ivins, Z. Martinec, and D. Wolf (2007), Models of active glacial isostasy roofing warm subduction: Case of the South Patagonian Ice Field, *J. Geophys. Res.*, *112*, B09405, doi:10.1029/2006JB004818.

Lemke, P., et al. (2007), Observations: Changes in snow, ice and frozen ground, in *Climate Change 2007: The Physical Science Basis. Contribution of Working Group I to the Fourth Assessment Report of the Intergovernmental Panel on Climate Change*, edited by S. Solomon et al., pp. 337–383, Cambridge Univ. Press, New York.

Lombard, A., D. Garcia, G. Ramillien, A. Cazenave, R. Biancale, J. M. Lemoine, F. Flechtner, R. Schmidt, and M. Ishii (2007), Estimation of steric sea level variations from combined GRACE and Jason-1 data, *Earth Planet. Sci. Lett.*, *254*(1–2), 194–202.

Milly, P. C. D., and A. B. Shmakin (2002), Global modeling of land water and energy balances. part I: The land dynamics (LaD) model, *J. Hydrometeorol.*, *3*(3), 283–299.

Ramillien, G., A. Lombard, A. Cazenave, E. R. Ivins, M. Llubes, F. Remy, and R. Biancale (2006), Interannual variations of the mass balance of the Antarctica and Greenland ice sheets from GRACE, *Global Planet. Change*, *53*(3), 198–208.

Raymond, C., T. Neumann, E. Rignot, K. Echelmeyer, A. Rivera, and G. Casassa (2005), Retreat of Tyndall Glacier, Patagonia, over the last half century, *J. Glaciol.*, *51*(173), 239–247.

Rignot, E., A. Rivera, and G. Casassa (2003), Contribution of the Patagonia ice fields of South America to sea level rise, *Science*, *302*(5644), 434–437, doi:10.1126/science.1087393.

Rivera, A., and G. Casassa (1999), Volume changes on Glacier Pio XI, Patagonia: 1975–1995, *Global Planet. Change*, *22*(1–4), 233–244.

Rivera, A., and G. Casassa (2004), Ice elevation, areal, and frontal changes of glaciers from National Park Torres del Paine, Southern Patagonia Icefield, *Arct. Antarct. Alp. Res.*, *36*(4), 379–389.

Swenson, S., and J. Wahr (2006), Post-processing removal of correlated errors in GRACE data, *Geophys. Res. Lett.*, *33*, L08402, doi:10.1029/2005GL025285.

Tamisiea, M. E., E. W. Leuliette, J. L. Davis, and J. X. Mitrovica (2005), Constraining hydrological and cryospheric mass flux in southeastern Alaska using space-based gravity measurements, *Geophys. Res. Lett.*, *32*, L20501, doi:10.1029/2005GL023961.

Tapley, B. D., S. Bettadpur, M. Watkins, and C. Reigber (2004), The gravity recovery and climate experiment: Mission overview and early results, *Geophys. Res. Lett.*, *31*, L09607, doi:10.1029/2004GL019920.

Velicogna, I., and J. Wahr (2006), Measurements of time-variable gravity show mass loss in Antarctica, *Science*, *311*(5768), 1754–1756, doi:10.1126/science.1123785.

Wahr, J., S. Swenson, V. Zlotnicki, and I. Velicogna (2004), Time-variable gravity from GRACE: First results, *Geophys. Res. Lett.*, *31*, L11501, doi:10.1029/2004GL019779.

Warren, C. R., and D. E. Sudgen (1993), The Patagonia Icefields: A glaciological review, *Arct. Alp. Res.*, *25*(4), 316–331.

————————————

D. D. Blankenship, Institute for Geophysics, University of Texas at Austin, 10100 Burnet Road, PRC, Bldg. 196, Austin, TX 78758-4445, USA.

J. L. Chen and B. D. Tapley, Center for Space Research, University of Texas at Austin, 3925 W. Braker Lane, Suite 200, Austin, TX 78759-5321, USA. (chen@csr.utexas.edu)

E. R. Ivins, Jet Propulsion Laboratory, California Institute of Technology, MS 300-233, 4800 Oak Grove Drive, Pasadena, CA 91109-8099, USA.

C. R. Wilson, Department of Geological Sciences, University of Texas at Austin, 1 University Station C1100, Austin, TX 78712-0254, USA.